

Article

Study on the Measurability of Gear Analytical Parameters in Double-Flank Measurement

Xiaoyi Wang ^{1,2,*}, Mingkang Liu ¹, Tianyang Yao ¹, Kunlei Zheng ¹, Chengxiang Zhao ¹, Longyuan Xiao ¹ and Dongjie Zhu ¹

¹ School of Mechatronics Engineering, Henan University of Science and Technology, Luoyang 471003, China; kklmk163@163.com (M.L.); yty0101@139.com (T.Y.); zk115538694420@163.com (K.Z.); zcx_98@126.com (C.Z.); xly15137615751@163.com (L.X.); zdjwsbn@163.com (D.Z.)

² Henan Key Laboratory of Mechanical Design and Transmission System, Henan University of Science and Technology, Luoyang 471003, China

* Correspondence: wxy2.0@163.com

Abstract: Double-flank measurement is the most commonly used full inspection method on the shop floor. However, the double-flank measurement method cannot measure analytical parameters such as pitch deviations and profile deviations, and this limitation is a pain point in the field of gear measurement. This paper studies the measurability of the analytical parameters of gears based on the results of double-flank measurement, proposes the definition of measurable area, and gives the relationship between the size of the measurable area and the number of teeth and the pressure angle and the gear error. Digital simulation methods were used to conduct measurement experiments on gear analytical parameters. In the experiments, the measurability of the analytical parameters of gears with various typical profile deviations in the double-flank measurement process was verified and analyzed. The test results show that not all profile deviations are unmeasurable in the process of double-flank measurement, but there exists a profile region in which the analytical parameters of the gear can be measured accurately. The size of the measurable area of the profile is mainly determined by the number of teeth and pressure angle of the gear, while the pitch deviations are always measurable under normal conditions.

Keywords: gear metrology; double-flank measurement; analytical parameters; measurable area; profile



Citation: Wang, X.; Liu, M.; Yao, T.; Zheng, K.; Zhao, C.; Xiao, L.; Zhu, D. Study on the Measurability of Gear Analytical Parameters in Double-Flank Measurement. *Sensors* **2023**, *23*, 9728. <https://doi.org/10.3390/s23249728>

Academic Editor: Manuchehr Soleimani

Received: 8 October 2023

Revised: 24 November 2023

Accepted: 4 December 2023

Published: 9 December 2023



Copyright: © 2023 by the authors. Licensee MDPI, Basel, Switzerland. This article is an open access article distributed under the terms and conditions of the Creative Commons Attribution (CC BY) license (<https://creativecommons.org/licenses/by/4.0/>).

1. Introduction

Mass-produced automobile gears and household product gears are irreplaceable in the national economy and national defense construction. Gear measurement plays an important role in gear quality control. Gear measurement can be categorized into composite measurement and analytical measurement. Analytical measurement is mainly used to acquire pitch deviations, profile deviations, and helix deviations, which are mainly used to analyze the source of process error. Meanwhile, composite measurement is mainly used to judge whether the product is qualified [1,2].

For the quality control of mass-produced gears, the double-flank composite test is the most commonly used inspection method [3,4]. In the field of gear measurement, it is generally believed that based on gear double-flank measurement, analytical parameters, such as pitch deviations, profile deviations, and helix deviations, cannot be obtained, and only radial composite parameters can be obtained [5–7]. If the analytical parameters can be obtained based on gear double-flank measurements, the double-flank measurement will be much more valuable, and both low cost and high performance will be realized, which can control the quality of gears well, reduce the cost of inspection, and increase the competitiveness of the enterprise's products.

The literature [8] improves the gear selecting machine by the use of the gear double-flank meshing measurement principle to measure parameters such as gear defects and

runout. The literature [9] analyzes the effect of the radial deformation of gears under the action of measuring force in double-flank measurement and proposes relevant algorithms to enhance the accuracy of the evaluation. The literature [10] developed a cloud processing system for gear double-flank meshing measurements to improve the utilization of information. In addition, there is a large amount of literature related to the measurement of double meshed gears, mainly focusing on how to improve the measurement accuracy and measurement efficiency [11–15]. Aiming at obtaining analytical parameters such as pitch deviations and profile deviations from gear double-flank measurement, some scholars have carried out research from different perspectives, and some progress has been made.

References [16,17] propose a method that uses a single tooth rack probe for radial comprehensive measurement, which can obtain the tooth profile deviations and pitch deviations of the left and right flanks of the tested gear, providing a way to measure the multiple parameters of gear accuracy simultaneously. Through further research on double-flank measurement based on rack-type probes, the literature [18] describes the double-flank rack probe (DFRP) method for the measurement of pitch and profile deviations of left and right tooth flanks and develops a gear measurement device based on the DFRP method. The literature [7] proposes a double-flank multi-dimensional measurement principle for gears, and an on-line gear measuring machine developed based on this principle can simultaneously obtain the radial comprehensive deviation and helical deviations of the measured gear. The models of radial and tangential errors in the double-flank test process were established in the literature [19], and the profile deviations and pitch deviations imported by the base circle radius deviations were simulated and measured based on the rack probe.

However, in the above studies, due to the use of rack-type probes or special probes, a conventional double-flank rolling tester cannot be used, and specialized measuring instruments need to be developed. The use of a single tooth rack-type probe cannot achieve continuous rotation measurement (like the conventional double-flank rolling test), and the efficiency is low when measuring gears with a large number of teeth. In conclusion, the existing double-flank rolling tester using a gear-shaped master gear cannot obtain analytical parameters such as pitch deviations and profile deviations.

In this paper, a new structure of the double-flank rolling tester is proposed, which adds two angle sensors to the conventional double-flank rolling tester and utilizes the master gear as a probe, which can realize the measurement of analytical parameters such as pitch deviations and partial profile deviations.

Firstly, based on the new double-flank rolling tester, this paper analyzes the measurability of analytical parameters in double-flank measurement. Secondly, the relationship between the basic parameters of the gear pair, profile deviations, and the size of the profile region of the measurable analytical parameter is explored. Finally, the measurement test of the analytical parameters in double-flank measurement was carried out by using the simulation method, which verified the measurability of the analytical parameters in double-flank measurement under a variety of profile deviation conditions.

2. Measurability Analysis

In order to achieve the measurement of analytical parameters based on the double flank, two angle sensors need to be added to the conventional double-flank instrument with some changes in the structure of the instrument. On the basis of the instrument, the measurability of the analytical parameters of the double-flank measurement using the master gear is explored, and a calculation method for the size and position of the profile area in which the analytical parameters can be obtained in the process of double-flank meshing of the gear is attained. Further, the relationship between the size of the measurable area of the analytical parameters of the product gear and the number of teeth and pressure angle of gears, as well as the relationship between the measurable area of the analytical parameters and the profile error, was explored and obtained.

2.1. Instrument

Figure 1 shows a double-flank rolling tester that allows analytical parameters to be obtained. Unlike a conventional double-flank tester, the new tester is equipped with an angle measuring system composed of two angle encoders attached to two axes of a master gear and measured gear, respectively. As with the conventional double-flank rolling tester, there is a spring loading device and a sensor for measuring the center distance. Compared with a conventional double-flank rolling tester, the fit between the shaft and the gear has been changed from the clearance fit to the tight fit. In order to increase the efficiency of gear replacement, it is an option to use an expandable arbor to fix the product gears.

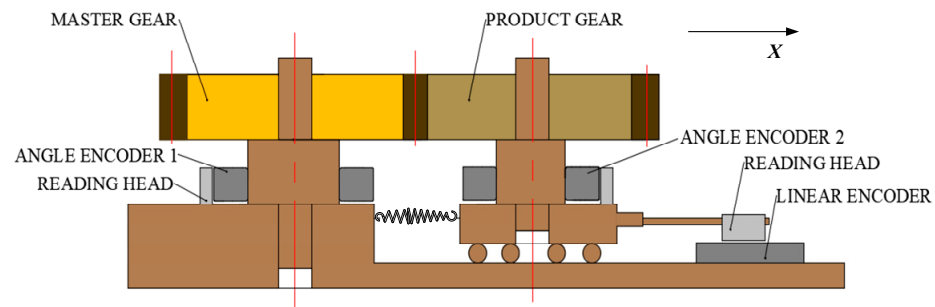


Figure 1. Schematic diagram of a double-flank rolling tester for obtaining analytical parameters.

In the measurement device shown in Figure 1, the master gear drives the angle encoder 1. The product gear rotates coaxially with the angle encoder 2 and shifts along the X-axis. The rotation angles are measured by two angle encoders, and the X-axis displacement is measured by a linear encoder. Based on the information on the two angles and one displacement measured by three sensors, the gear analytical parameters can be obtained, and then the gear accuracy grade of the corresponding parameters can be evaluated.

2.2. Analysis

In this paper, the measurability of analytical parameters of involute cylindrical gears is studied. The analytical methods for other types of gears are similar.

According to the gear geometry, the transverse base pitch Pb and the contact ratio ε of double-flank meshed gear pairs can be obtained from Equations (1) and (2),

$$Pb = \pi m \cdot \cos(\alpha_0) \quad (1)$$

$$\varepsilon = (z_1 \cdot (\tan(\alpha_{a1}) - \tan(\alpha_0)) + z_2 \cdot (\tan(\alpha_{a2}) - \tan(\alpha_0))) / (2\pi) \quad (2)$$

where α_0 is the transverse pressure angle, m is the modulus, and z_1 and z_2 are the number of teeth on the master gear and the product gear, respectively. α_{a1} and α_{a2} are the pressure angles on the tip diameter of the master gear and the product gear, respectively.

As shown in Figure 2, taking the gear parameters in Table 1 as an example, the master gear is the driving gear and the product gear is the driven gear, and both gears are standard gears; the contact ratio is less than 2. Points A and B on the path of contact are the tangent points between the path of contact and the base circle of the master gear and the product gear, respectively. Points P_1 and P_2 are the intersection of the tip circle of the product gear with the path of contact and the intersection of the tip circle of the master gear with the path of contact, respectively. Points C_1 and C_2 are the demarcation points where the instantaneous contact ratio changes during the meshing process. Point P is the pitch point of the two gears.

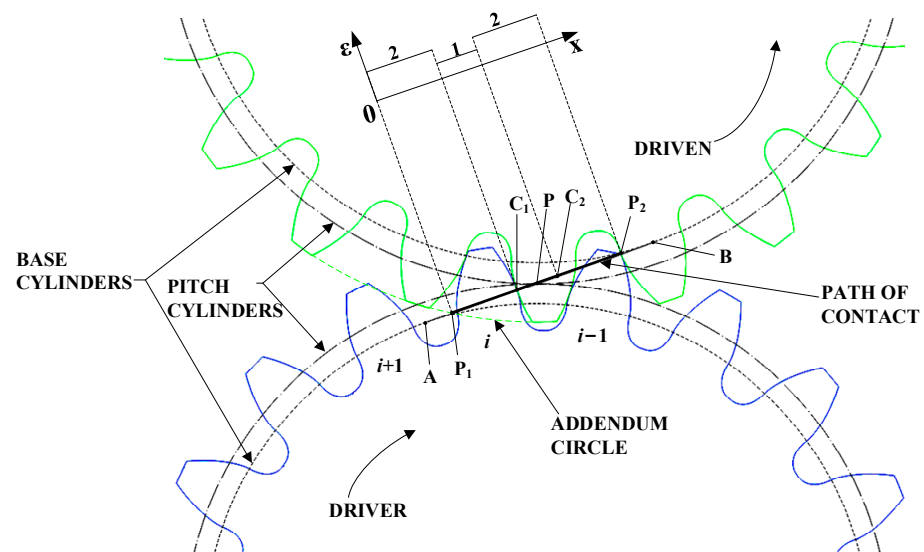


Figure 2. Relation between the path of contact and instantaneous contact ratio of gears.

Table 1. Gear parameters in the experiments.

Parameter	Modulus (mm)	Number of Teeth	Transverse Pressure Angle (eg)	Profile Shift Coefficient
Product gear	2	20	20	0
Master gear	2	19	20	0

From the geometric relationship in Figure 2 and the definition of contact ratio, it can be concluded that

$$\begin{cases} P_2C_1 = P_1C_2 = Pb \\ P_1P_2 = Pb \cdot \varepsilon \end{cases} \quad (3)$$

where P_2C_1 , P_1C_2 , and P_1P_2 are the lengths of the corresponding line segments on the path of contact in Figure 2. From the geometrical relationship in Figure 2 and Equation (3), the following can be calculated:

$$P_1C_1 = P_2C_2 = P_1P_2 - P_2C_1 = Pb \cdot (\varepsilon - 1) \quad (4)$$

where P_1C_1 and P_2C_2 are the lengths of the corresponding line segments on the path of contact in Figure 2. Then

$$C_1C_2 = P_2C_1 - P_2C_2 = Pb \cdot (2 - \varepsilon) \quad (5)$$

As shown in Figure 2, during the double-flank meshing process, the number of pairs of teeth in instantaneous meshing will change regularly. From Equations (4) and (5), the regions P_1C_1 and P_2C_2 on both sides of P_1P_2 are the corresponding double-flank meshing regions [20], where the instantaneous contact ratio of the corresponding flanks is two. When the actual meshing points are located in the region of P_1C_1 and P_2C_2 , the gear double-flank measurements are obtained as a result of the combined profile deviations of corresponding flanks on both teeth. Then, the profile regions corresponding to the P_1C_1 and P_2C_2 are defined as “unmeasurable areas”. The region C_1C_2 is the single corresponding flank meshing region, where the instantaneous contact ratio of corresponding flanks is one. When the instantaneous meshing point is within C_1C_2 , the deviations of the gear double-flank measurements are determined by the profile deviations of a single tooth flank, so the measured error directly reflects the profile deviations of the flank. The profile regions corresponding to C_1C_2 are defined as “measurable areas”. In this area, the profile deviations are obtainable, and then the pitch deviations can be calculated.

Figure 3 is a schematic diagram of the three states of the instantaneous contact ratio variation. In Figure 3, the product gear meshes with the master gear sequentially at the $i - 1$ th, i th, and $i + 1$ th teeth. The master gear is the driving gear and rotates clockwise. The product gear is the driven gear and rotates counterclockwise. Figure 3a shows the state in which the right tooth flanks of the i th tooth and the $i - 1$ th tooth of the master gear are engaged at the same time, which corresponds to the P_1C_1 region in Figure 2. Figure 3b shows the state where only the right tooth flank of the i th tooth participates in meshing in the right tooth flank of the master gear, which corresponds to the C_1C_2 region in Figure 2. Figure 3c shows the state in which the right tooth flanks of the i th tooth and the $i + 1$ th tooth of the master gear engage at the same time, which corresponds to the P_2C_2 region in Figure 2.

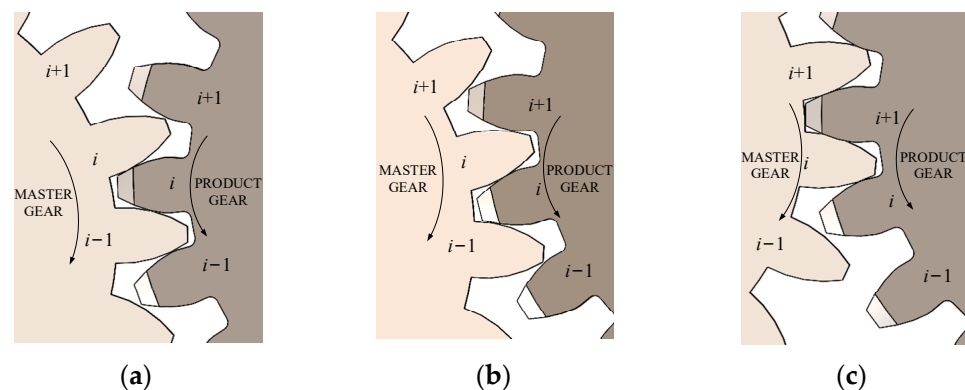


Figure 3. Schematic diagram of gear meshing states. (a) State 1: the instantaneous contact ratio of right flank is 2. (b) State 2: the instantaneous contact ratio of right flank is 1. (c) State 3: the instantaneous contact ratio of right flank is 2.

Taking the parameters of the master gear and the product gear shown in Table 1, according to the above definitions and Equations (6) and (7), the range of the measurable area can be calculated, as shown in Figure 4.

$$\begin{cases} BC_1 = BP_1 - P_1C_1 = r_b \cdot \tan(\alpha_{a2}) - Pb \cdot (\varepsilon - 1) \\ BC_2 = BP_1 - P_1C_1 - C_1C_2 = r_b \cdot \tan(\alpha_{a2}) - Pb \cdot (2 - \varepsilon) - Pb \cdot (\varepsilon - 1) \end{cases} \quad (6)$$

$$\begin{cases} \alpha_{C1} = \arctan\left(\frac{AC_1}{r_b}\right) \\ \alpha_{C2} = \arctan\left(\frac{AC_2}{r_b}\right) \end{cases} \quad (7)$$

where BC_1 , BC_2 , and BP_1 are the lengths of the corresponding line segments on the path of contact in Figure 2, r_b is the radius of the base circle of the product gear, and α_{C1} and α_{C2} are the pressure angles of the product gear corresponding to points C_1 and C_2 , respectively.

From the above equations, the pressure angle range of the measurable area is $(16.398^\circ, 23.531^\circ)$, as shown in Figure 4. The unmeasurable area is divided into two parts, which are on both sides of the measurable area.

2.3. Geometric Factors Affecting the Measurable Area

The size of the measurable area of the analytical parameters is related to the basic parameters of the master gear and the product gear. The number of teeth and the pressure angle are the main parameters that affect the size of the measurable area. In transmission, the modulus of two gears is usually equal, and the change in the modulus is equivalent to proportionally increasing or decreasing the size of the gear. Therefore, the module is not the main parameter that affects the size of the measurable area.

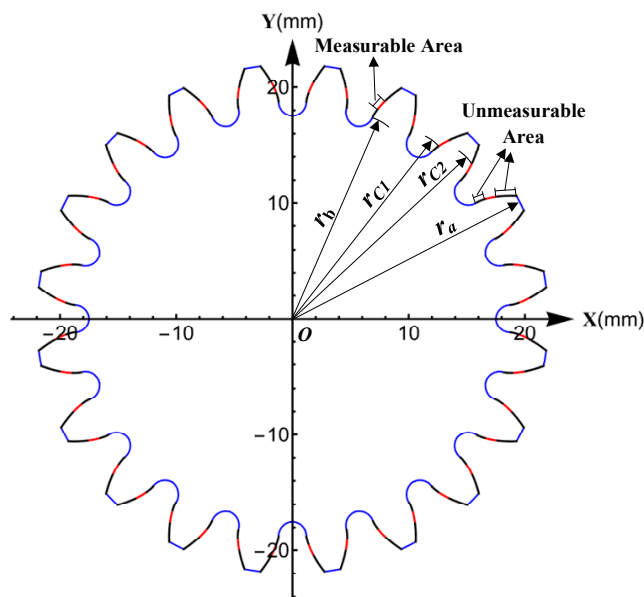


Figure 4. The distribution of measurable and unmeasurable areas on the profiles of the product gear.

The proportion of the measurable area to the entire meshing area of profile can be calculated with reference to the radius or with reference to the roll length. In this paper, the proportion of the measurable area (P_{ma}) over the entire profile meshing region is defined as

$$P_{ma} = (r_{C2}(z_1, z_2, \alpha_0) - r_{C1}(z_1, z_2, \alpha_0)) / (r_a - r_b(z_2, \alpha_0)) \tag{8}$$

where r_{C1} and r_{C2} are the radius of the points on the profile of the product gear corresponding to points C_1 and C_2 in Figure 2, r_a is the radius of the tip circle of the product gear, and r_b is the radius of the base circle of the product gear. Among them, r_{C2} and r_{C1} change with z_1, z_2 and α_0 , r_b changes with z_2 and α_0 .

The relationship between the number of teeth and the proportion of measurable area is shown in Figure 5. The P_{ma} , between 15% and 35%, corresponds to the variation in the number of teeth of the master gear between 10 and 40 and the variation in the number of teeth of the product gear between 17 and 40. The percentages are larger when the number of teeth is smaller. The maximum percentage occurs at $z_1 = 10$ and $z_2 = 17$, with a percentage of 35%.

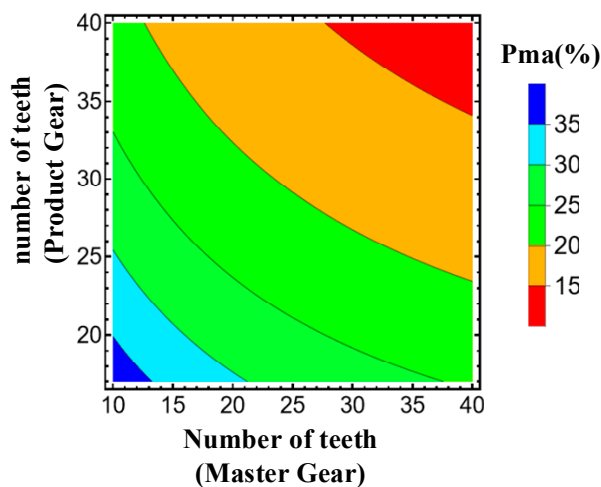


Figure 5. Relationship between the number of teeth and the proportion of measurable area ($\alpha_0 = 20^\circ$).

It can be seen that in some cases, analytical parameters including profile deviations and pitch deviations can be extracted from the double-flank measurements, thus providing a basis for the analysis and evaluation of process errors in gear manufacturing.

Further, in order to investigate the effect of pressure angle variation on the size of the measurable area, analyses were conducted at pressure angles of 15° and 25° , and the results are shown in Figure 6. It can be seen that the larger the transverse pressure angle, the greater the percentage of the measurable area in the profile.

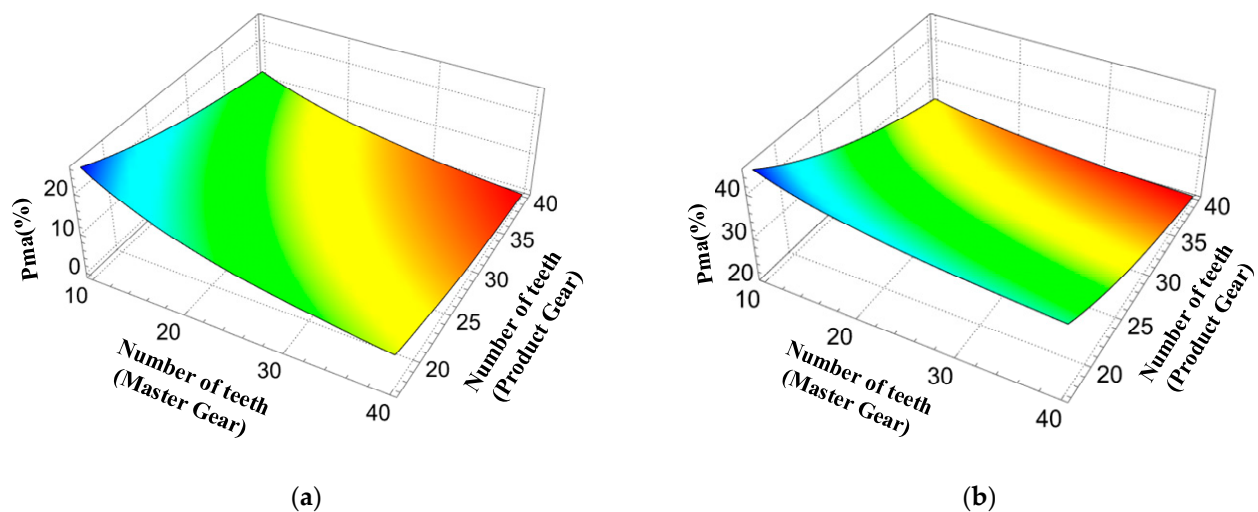


Figure 6. Relationship between the number of teeth and the proportion of measurable area for transverse pressure angles of 15° and 25° . (a) $\alpha_0 = 15^\circ$. (b) $\alpha_0 = 25^\circ$.

Under the condition of keeping the number of teeth of the product gear and the master gear at 19 and 20 (the number of teeth in Table 1), respectively, changing the transverse pressure angle of the two gears from 15° to 30° results in the change curve of P_{ma} as shown in Figure 7. As the transverse pressure angle becomes larger, the proportion of the measurable area to the whole profile area also becomes larger, which is a nonlinear relationship.

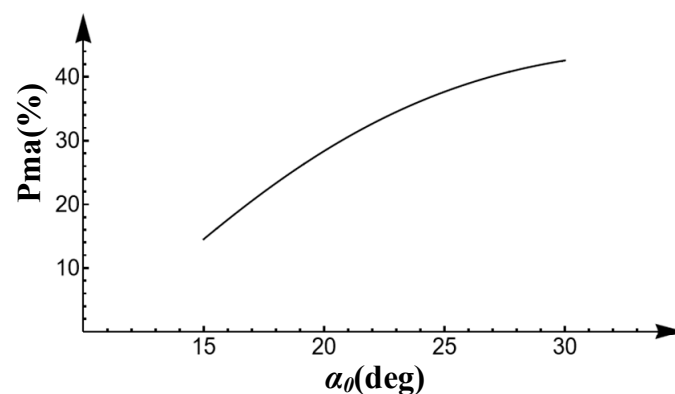


Figure 7. Proportion of measurable area for transverse pressure angle from 15° to 30° ($z_1 = 19, z_2 = 20$).

3. Experiments and Analysis

In order to verify the measurability of the analytical parameters in the measurable area in the double-flank measurement, various typical profile deviations were used as the profile deviations for the $i - 1$ th, i th, and $i + 1$ th tooth. Based on the gear parameters in Table 1 and the principle of the double-flank rolling tester in Figure 1, the simulation of the double-flank measurement results was conducted. Furthermore, the information on the center distance variation and the two angles from the double-flank measurement results was utilized to solve the analytical parameters [21].

3.1. Typical Profile Deviations

Typical profile deviations can be categorized into zero-order translation error (Figure 8a), first-order inclination error (Figure 8b), second-order parabolic error (Figure 8c), and higher-order sinusoidal error (Figure 8d). Superposition of the profile deviations of each order can produce a spline-type error curve close to the actual gear profile deviations in Figure 8e,f.

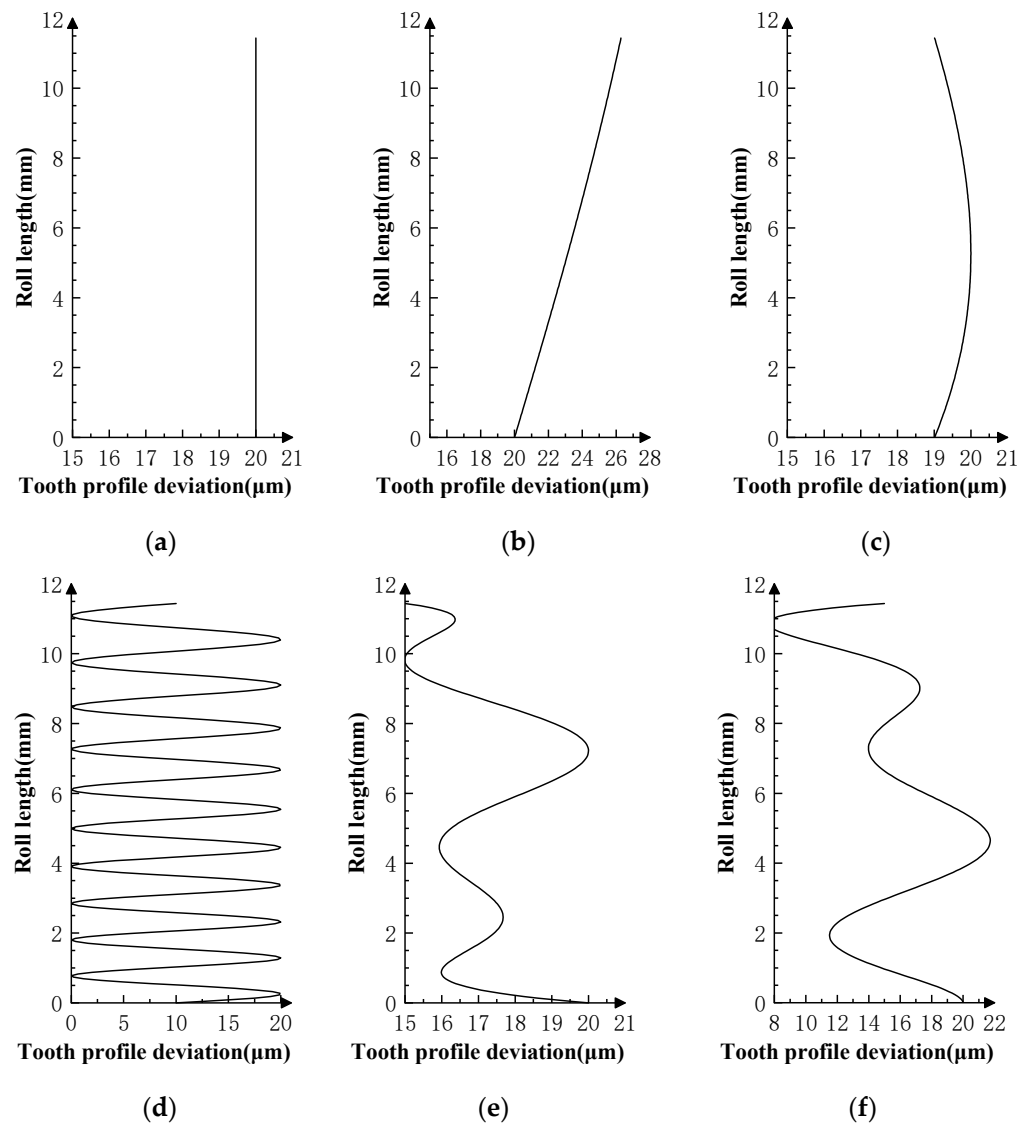


Figure 8. Type of profile deviations for simulations. (a) Zero-order error curve. (b) First-order error curve. (c) Second-order parabolic error curve. (d) Higher-order sinusoidal error curve. (e) Spline-type error curve I. (f) Spline-type error curve II.

3.2. Results and Analysis

Various typical profile deviations were superimposed on three successive corresponding flanks of the product gear, and several sets of tests were carried out. The theoretical profile deviations for the three teeth of $i - 1$ th, i th, and $i + 1$ th, together with the measurability test results, are shown in Figures 9–18. With the exception of Experiments V and VI, the magnitude of the profile deviations corresponds to the tolerance class 9 defined in ISO 1328-1 [22].

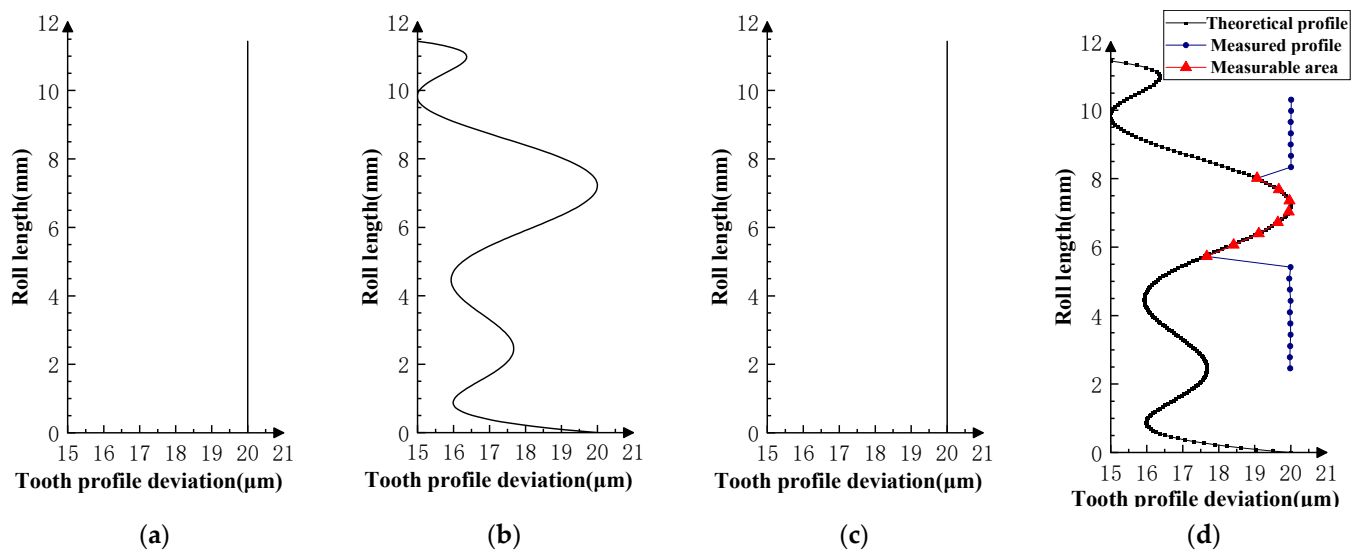


Figure 9. Experiment I (zero-order error for front and rear teeth). (a) Theoretical profile error of $i - 1$ th teeth. (b) Theoretical profile error of i th teeth. (c) Theoretical profile error of $i + 1$ th teeth. (d) Profile measurement results and measurable area.

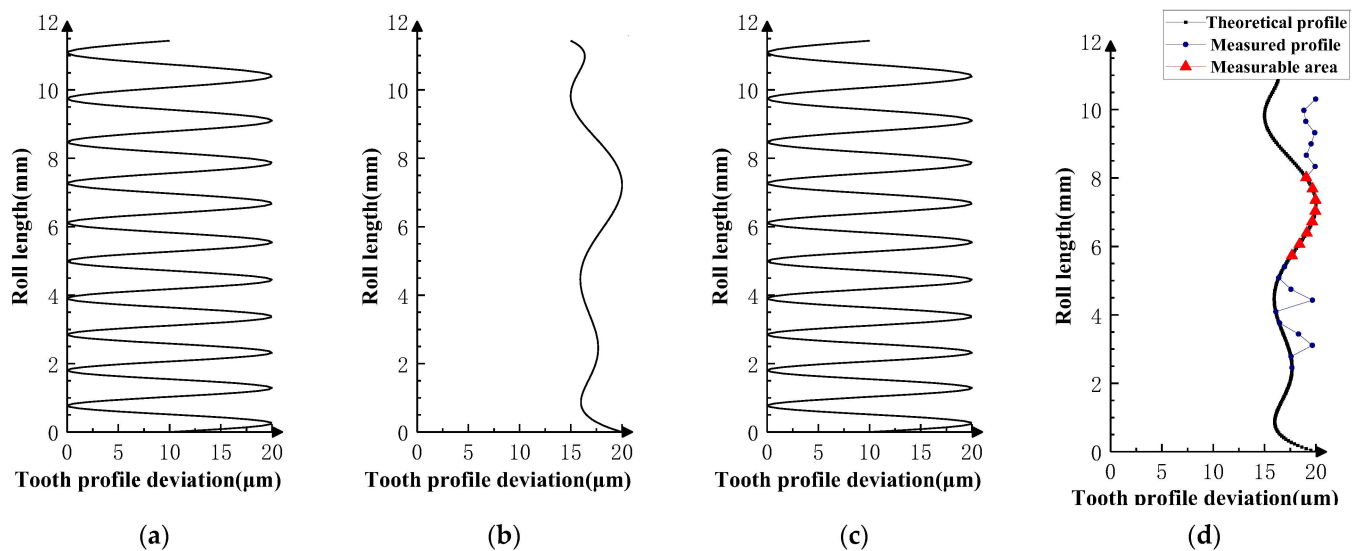


Figure 10. Experiment II (higher-order error for front and rear teeth). (a) Theoretical profile error of $i - 1$ th teeth. (b) Theoretical profile error of i th teeth. (c) Theoretical profile error of $i + 1$ th teeth. (d) Profile measurement results and measurable area.

In Experiment I, the front and rear teeth are with zero-order errors, while the i th tooth is with a spline error. In Experiment II, the front and rear teeth are with higher-order sinusoidal errors. In Experiment III, the front and rear teeth are with first-order errors. Experiment III was divided into three situations: the trend of front and rear tooth error increasing simultaneously, decreasing simultaneously, and having different trends. In Experiment IV, the front and rear teeth are with parabolic errors, and the i th tooth is with two types of spline errors, convex and concave.

The profile deviations of tooth $i - 1$ th and tooth $i + 1$ th in Experiment I, II, III, and IV are greater than or equal to that of tooth i th, but the magnitudes of the errors are basically equivalent, as shown in Figures 9–13. The measured profile deviations of the product gear are basically equal to the theoretical profile deviations of the tooth i th only in the measurable area, which verifies the measurability of the analytical parameters in the measurable area.

As shown in Figures 11–13, three sets of first-order error tests in Experiment III were conducted to investigate the effect of error on the measurement results. Among them, the measured profile deviations of the addendum and dedendum meshing zones of the i th tooth in the measurement results of Experiment III-2 have different inclination directions, indicating that the test results conform to a hidden rule that the theoretical profile deviations of the $i + 1$ th tooth mainly affect the dedendum meshing zone of the i th tooth, and the theoretical profile deviations of the $i + 1$ th tooth mainly affect the addendum meshing zone of the i th tooth.

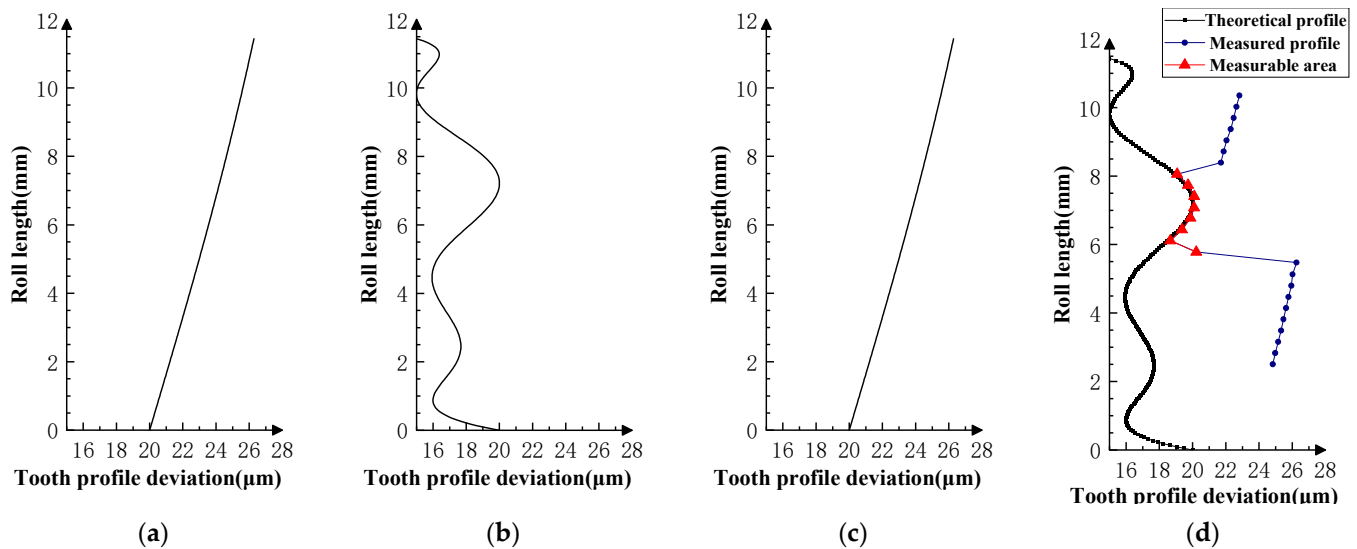


Figure 11. Experiment III-1 (the $i - 1$ st tooth is a first-order increasing error; the $i + 1$ st tooth is a first-order increasing error). (a) Theoretical profile error of $i - 1$ th teeth. (b) Theoretical profile error of i th teeth. (c) Theoretical profile error of $i + 1$ th teeth. (d) Profile measurement results and measurable area.

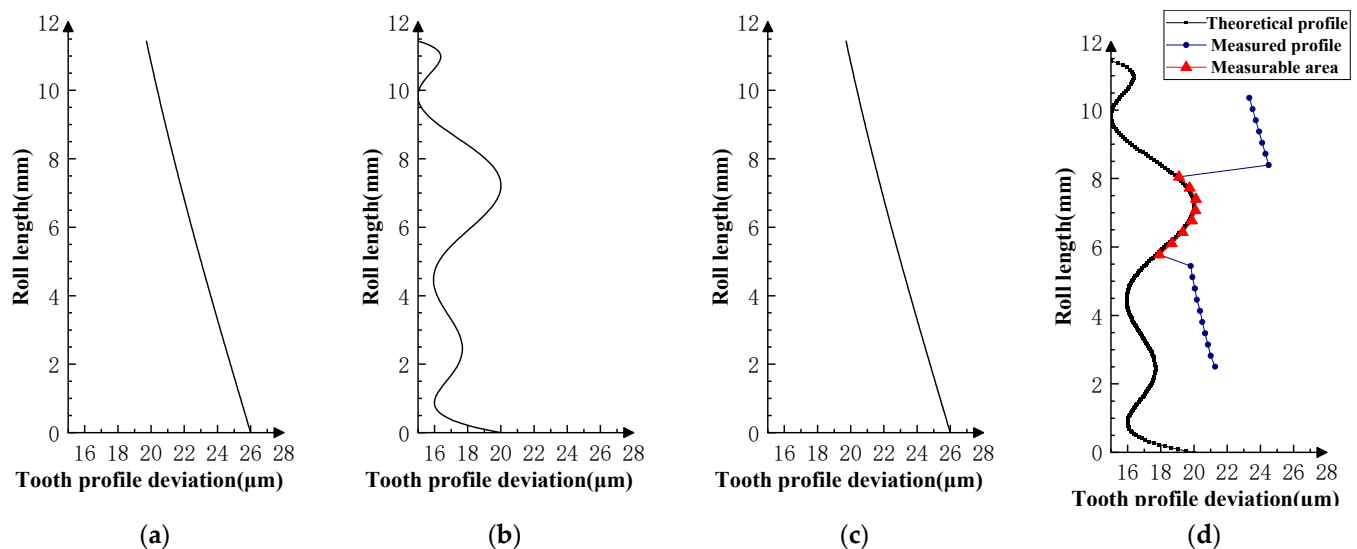


Figure 12. Experiment III-2 (the $i - 1$ st tooth is a first-order decreasing error, and the $i + 1$ st tooth is a first-order decreasing error). (a) Theoretical profile error of $i - 1$ th teeth. (b) Theoretical profile error of i th teeth. (c) Theoretical profile error of $i + 1$ th teeth. (d) Profile measurement results and measurable area.

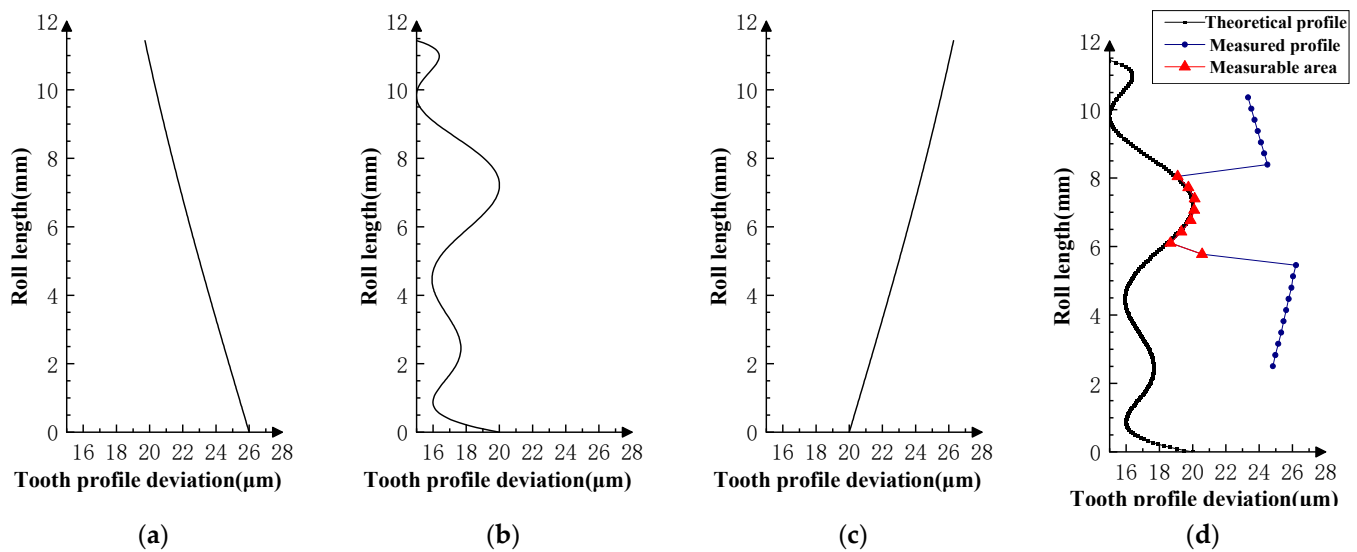


Figure 13. Experiment III-3 (the $i-1$ st tooth is a first-order increasing error, and the $i+1$ st tooth is a first-order decreasing error). (a) Theoretical profile error of $i-1$ th teeth. (b) Theoretical profile error of i th teeth. (c) Theoretical profile error of $i+1$ th teeth. (d) Profile measurement results and measurable area.

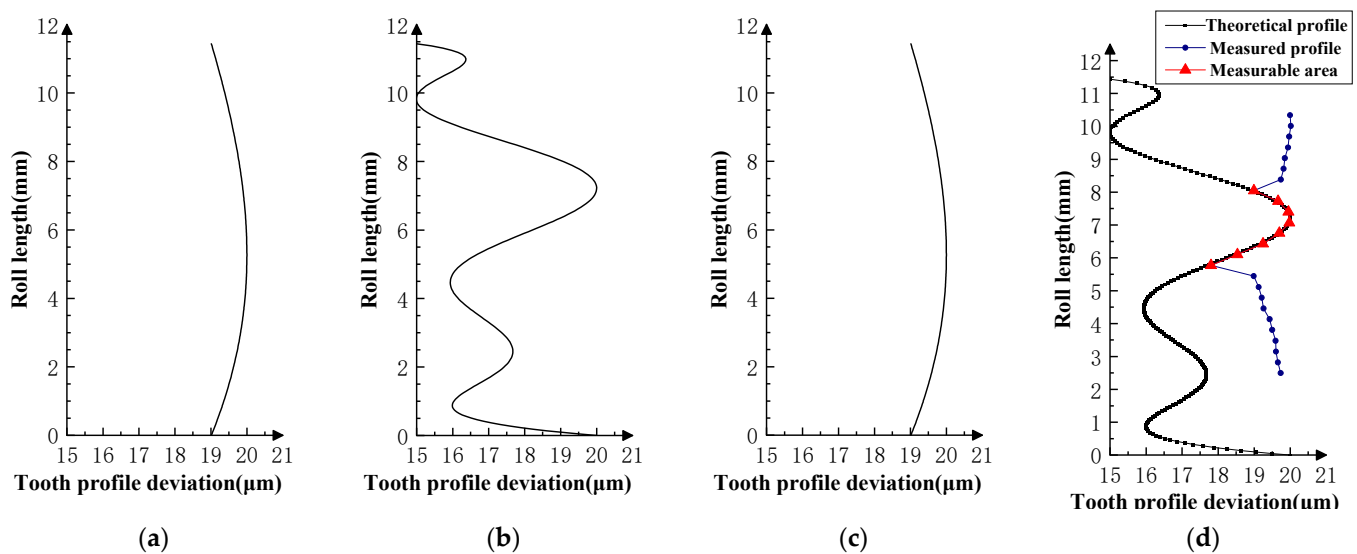


Figure 14. Experiment IV-1 (the $i-1$ st and $i+1$ st teeth are second-order errors, and the i -th tooth is the mid-convex spline curve error). (a) Theoretical profile error of $i-1$ th teeth. (b) Theoretical profile error of i th teeth. (c) Theoretical profile error of $i+1$ th teeth. (d) Profile measurement results and measurable area.

As shown in Figure 16, the profile deviations of the $i-1$ th and $i+1$ th teeth in Experiment V are smaller than that of the i th teeth, and the actual measurable area of the profile deviations is much larger than the theoretical measurable area, indicating that the measurable area can be enlarged by thinning the tooth flanks of the front and rear neighboring teeth of the master gear. This is similar to the role of the teeth-skipped gear (thinning gear) in the gear integrated error measurement [23–26].

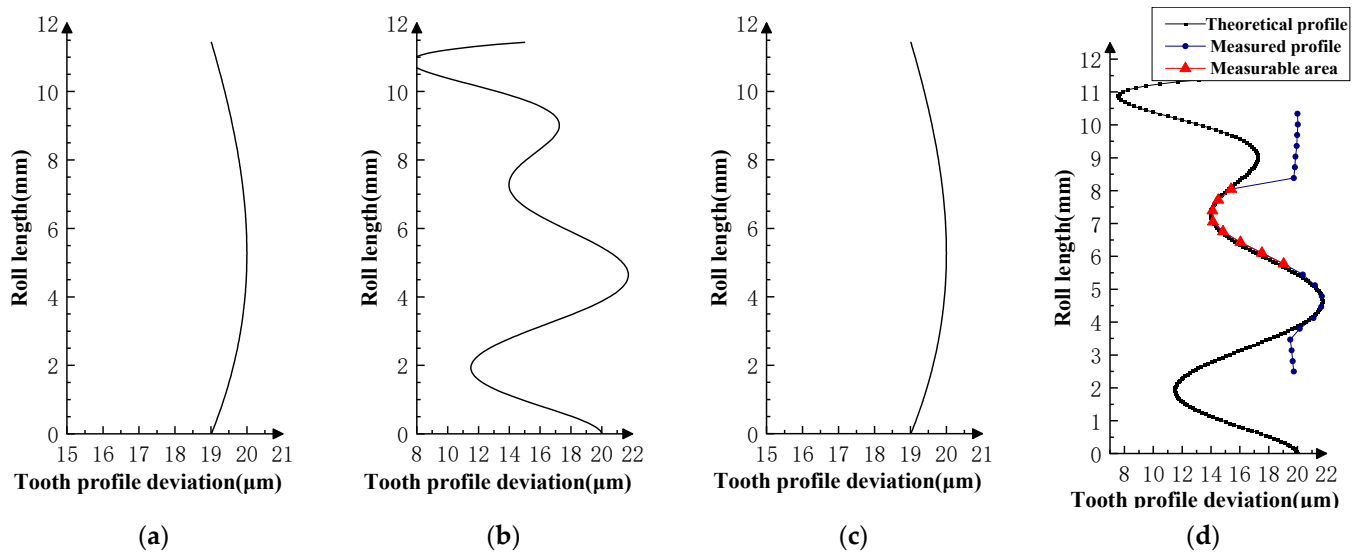


Figure 15. Experiment IV-2 (the $i - 1$ st and $i + 1$ st teeth are second-order errors, and the i -th tooth is the mid-concave spline curve error). (a) Theoretical profile error of $i - 1$ th teeth. (b) Theoretical profile error of i th teeth. (c) Theoretical profile error of $i + 1$ th teeth. (d) Profile measurement results and measurable area.

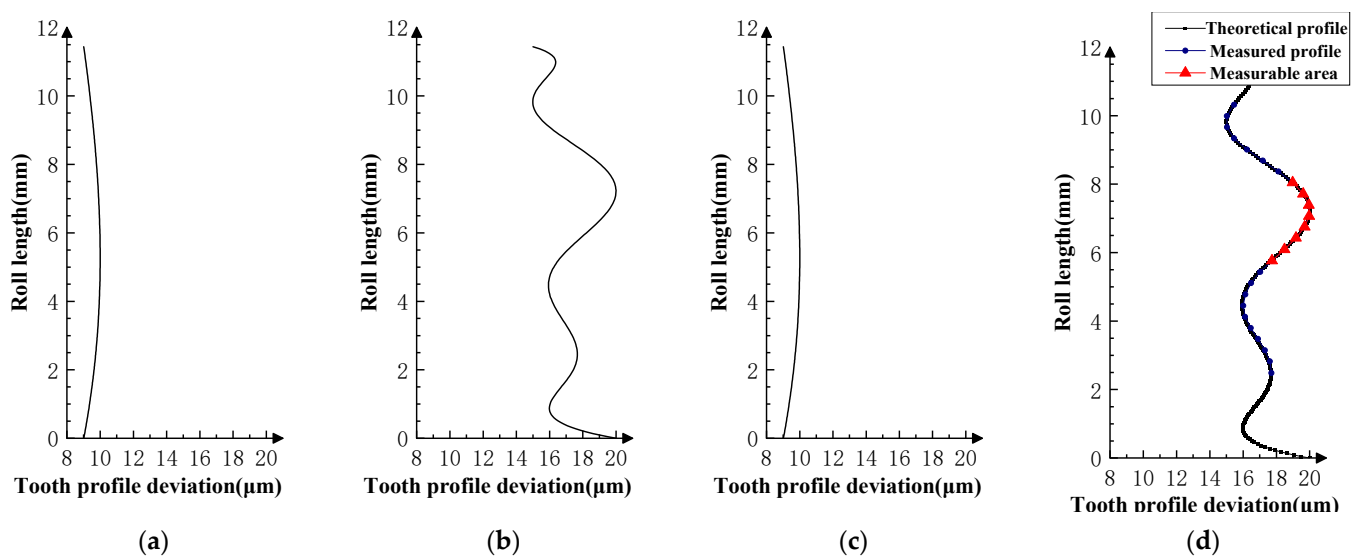


Figure 16. Experiment V (the $i - 1$ st and $i + 1$ st teeth are small magnitude second-order errors, and the i -th tooth is the mid-convex spline curve error). (a) Theoretical profile error of $i - 1$ th teeth. (b) Theoretical profile error of i th teeth. (c) Theoretical profile error of $i + 1$ th teeth. (d) Profile measurement results and measurable area.

As shown in Figures 17 and 18, the profile deviations of the $i - 1$ th and $i + 1$ th teeth in Experiment VI are much larger than that of the i th tooth; as the profile deviations of the $i - 1$ th and $i + 1$ th teeth gradually increase, the overlap area between the measured profile deviations and the theoretical profile deviations of the i th tooth gradually decreases. This shows that if the profile deviations of the neighboring tooth of the measured tooth are too large (the amplitude of the error in VI-2 is as high as $250 \mu\text{m}$), the profile deviations of the measured tooth will be impossible to measure in the double-flank measurement.

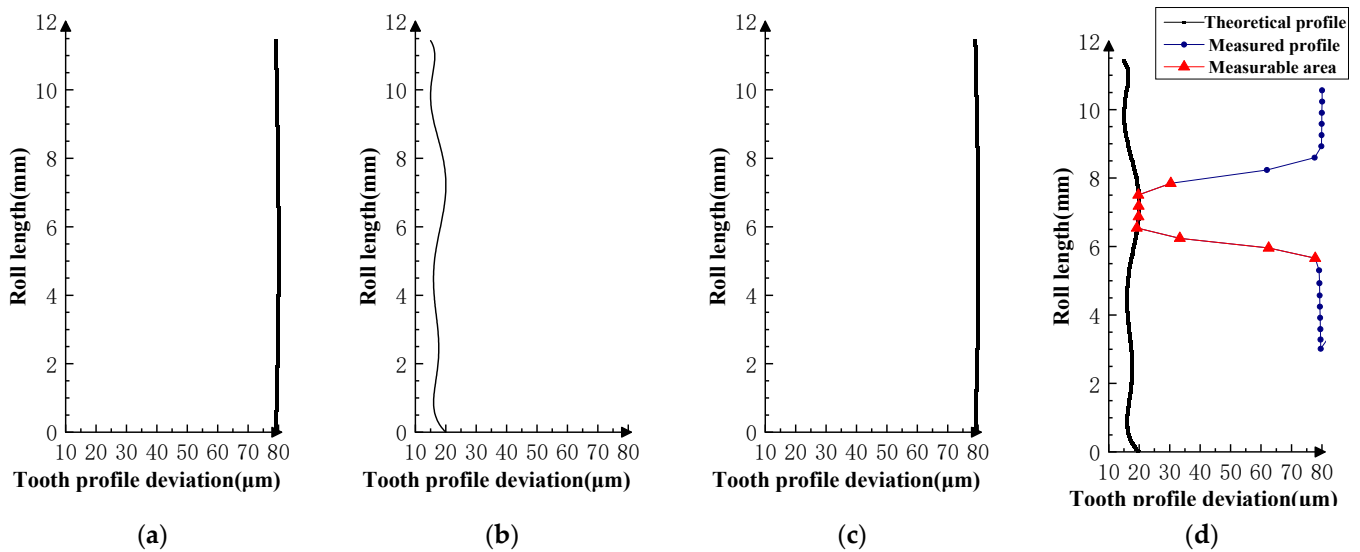


Figure 17. Experiment VI-1 (the $i - 1$ st and $i + 1$ st teeth are large-value second-order errors, and the i -th tooth is the mid-convex spline curve error). (a) Theoretical profile error of $i - 1$ th teeth. (b) Theoretical profile error of i th teeth. (c) Theoretical profile error of $i + 1$ th teeth. (d) Profile measurement results and measurable area.

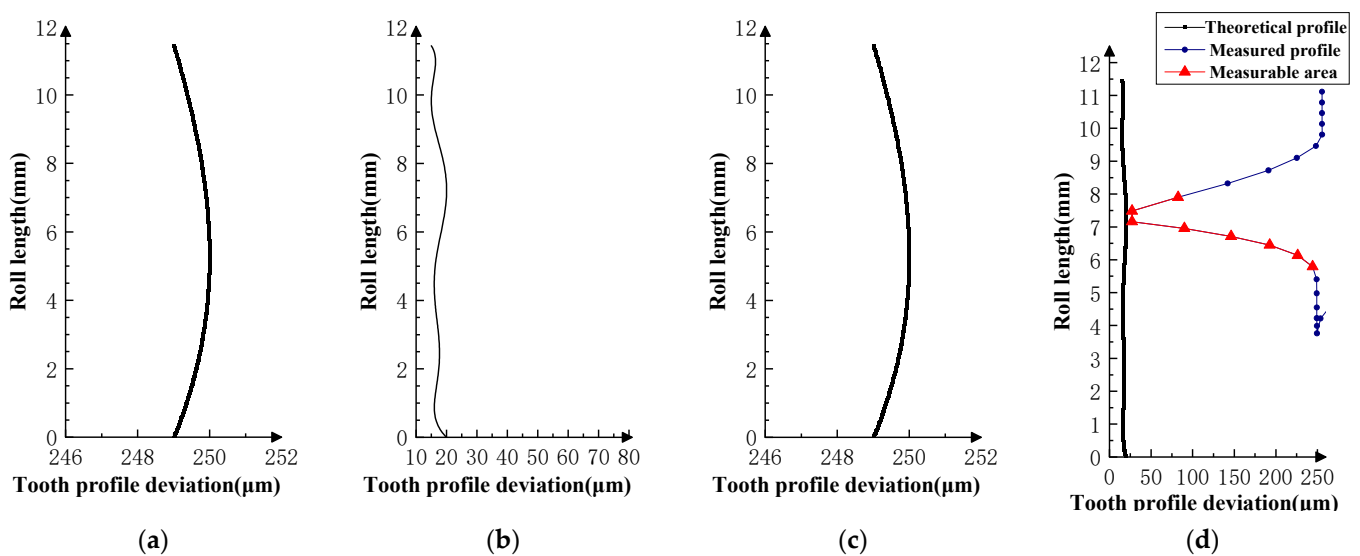


Figure 18. Experiment VI-2 (the $i - 1$ st and $i + 1$ st teeth are larger-value second-order errors, and the i -th tooth is the mid-convex spline curve error). (a) Theoretical profile error of $i - 1$ th teeth. (b) Theoretical profile error of i th teeth. (c) Theoretical profile error of $i + 1$ th teeth. (d) Profile measurement results and measurable area.

Through analysis of the experimental results, the size of the measurable area on the flank is related to the actual gear error. The type, magnitude, and shape of the error are factors that affect the size of the measurable area. Furthermore, some valuable assumptions can be made:

1. The size of the measurable area is mainly affected by the amplitude of the error (related to the accuracy grade of the gear); the larger the error and the lower the accuracy grade, the smaller the measurable area will be. However, when the gear accuracy is equal to or better than the medium accuracy level (grade 5–7 in ISO 1328-1), the size of the measurable area is basically determined by geometric factors.

2. When the profile deviations of the front and rear teeth are much larger than that of the measured flank, the measurable area will be smaller, as shown in Experiment VI (Figures 17 and 18).
3. When the profile deviations of the front and rear are smaller than that of the measured flank, the measurable area becomes larger. This is shown in Experiment V (Figure 16).
4. The size of the measurable area is basically independent of the type of profile deviations. Under the same amplitude conditions, different profile deviation types have no significant effect on the size of the measurable area.
5. The shape of the error of the same accuracy grade has no significant effect on the size of the measurable area. As in Experiment IV (Figures 14 and 15), the profile deviations of the measured tooth have two types of shapes in the measurable area, convex and concave, and there is no obvious change in the size of the measurable area under the two shapes.

4. Conclusions

This paper analyzes the measurability of analytical parameters in gear double-flank measurement. The definition of the measurable area of the analytical parameters in the double-flank measurement is presented, the calculation method of the size and position of the measurable area is proposed, the rule of the change in the size of the measurable area with the number of teeth and the pressure angle of the meshing gears is calculated, and the effect of the gear error on the measurable area is analyzed.

The experimental data show that the measurable area exists when the accuracy of product gear is class 9 or higher and when there are zero-order error, first-order error, second-order error, higher-order error, and spline error on the profile of the product gear.

The higher the accuracy of the product gear, the more stable the measurable area of the analytical parameters will be. When the product gear is of medium or higher accuracy (e.g., automotive gear), it is possible to accurately isolate the profile deviations of the measurable area based on the results of the double-flank measurement and then obtain the pitch deviations, radial runout, and so on.

This study of the measurability of the analytical parameters in double-flank measurement is based on a cylindrical spur gear pair. Similar studies can be carried out in the future on other types of gears, such as helical gears. In addition, the size of the measurable area is affected by the actual gear accuracy. The influence rules of gear deviations, such as pitch and helix deviations, are complicated and not discussed in this paper for the time being. The influence rules require further research in the future.

Author Contributions: Conceptualization, X.W. and M.L.; data curation, X.W. and M.L.; formal analysis, X.W. and M.L.; funding acquisition, X.W. and M.L.; investigation, X.W. and M.L.; methodology, X.W. and M.L.; project administration, X.W. and M.L.; resources, X.W., M.L., T.Y., K.Z., C.Z., L.X. and D.Z.; software, X.W. and M.L.; supervision, X.W. and M.L.; validation, X.W. and M.L.; visualization, X.W. and M.L.; writing—original draft, X.W. and M.L.; writing—review and editing, X.W. and M.L. All authors have read and agreed to the published version of the manuscript.

Funding: This research was funded by the National Natural Science Foundation of China (52227809, 51775172).

Institutional Review Board Statement: Not applicable.

Informed Consent Statement: Not applicable.

Data Availability Statement: The data that support the findings of this study are available from the corresponding author upon reasonable request.

Conflicts of Interest: The authors declare no conflict of interest.

References

1. Goch, G.; Guenther, A.; Peng, Y.; Ni, K. Gear metrology—An update. *CIRP Ann.* **2023**, *72*, 725–751. [[CrossRef](#)]
2. Shi, Z.; Fei, Y.T.; Xie, H.K. 100 years of gear measurement technology—Review & prospect. *Eng. Sci.* **2003**, *5*, 13–17.

3. Zhang, B. *Modern Measurement Technology and Instruments for Gears*; China Machine Press: Beijing, China, 1986.
4. Pueo, M.; Santolaria, J.; Acero, R.; Gracia, A. A review of tangential composite and radial composite gear inspection. *Precis. Eng.* **2017**, *50*, 522–537. [[CrossRef](#)]
5. Frazer, R.C.; Bicker, R.; Cox, B.; Harary, H.; Haertig, F. An international comparison of involute gear profile and helix measurement. *Metrologia* **2003**, *41*, 12. [[CrossRef](#)]
6. Rudolf, O. History of gear measuring machines and traceability 1900–2006. *Gear Prod. News* **2006**, *10*, 20–25.
7. Shi, Z.; Tang, J.; Wei, H.; Gao, Y.; Liu, C. Gear in-line measuring machine based on double-flank gear rolling test with multi-degrees of freedom. *Chin. J. Sci. Instrum.* **2009**, *30*, 303–307.
8. Kawasaki, Y.; Shinoda, M.; Nojiri, S.; Hayashi, A.; Hoshi, T. Development of a new automatic gear selecting machine for automobile transaxle manufacturing. *CIRP Ann.* **1984**, *33*, 363–368. [[CrossRef](#)]
9. Tang, J.; Yang, B.; Shi, Z. Influence on center distance by measurement force in double-flank gear rolling test. *Measurement* **2021**, *168*, 108321. [[CrossRef](#)]
10. Tang, J.; Zhang, R.; Shi, Z. Deployment and implementation of data cloud processing system for double-flank gear rolling test based on javaweb. *Guangxue Jingmi Gongcheng/Opt. Precis. Eng.* **2021**, *29*, 1387–1396. [[CrossRef](#)]
11. Pommer, A. *Gear Rollscan for High Speed Gear Measurement*; AGMA: Alexandria, VA, USA, 2002.
12. Bai, S. Design and Development of the Measurement System of Double Flank Gear Roll Tester Based on Statistical Process Control. Master's Thesis, Xi'an University of technology, Xi'an, China, 2020.
13. Jiang, M.; Tang, J.; Shi, Z. Development of measurement uncertainty evaluation software for double flank worm gear pair rolling tester. *Meas. Control. Technol.* **2022**, *41*, 109–115.
14. Liu, Q. Improvement of mechanical gear double-flank meshing comprehensive measuring instrument. *Metrol. Sci. Technol.* **2005**, *3*, 62–64.
15. Xu, T. Software Development of Automatic Double Flank Meshing Instrument Based on Motion Controller. Master's Thesis, Xi'an Technological University, Xi'an, China, 2019.
16. Zhang, Z. Simultaneous measurement the profile deviations the left and right tooth flank. *Metrol. Meas. Tech.* **1994**, *21*, 4–7.
17. Zhang, Z. Simultaneously measuring the pitch deviations of the left and right tooth flank. *Metrol. Meas. Tech.* **1995**, *22*, 10–12.
18. Tang, J.; Jia, J.; Fang, Z.; Shi, Z. Development of a gear measuring device using dfrp method. *Precis. Eng.* **2016**, *45*, 153–159. [[CrossRef](#)]
19. Tang, J.; Zhang, Y.; Shi, Z. Radial and tangential error analysis of double-flank gear measurement. *Precis. Eng.* **2018**, *51*, 552–563. [[CrossRef](#)]
20. Yu, S.; Liu, H.; Pan, J.; Huang, Y. Study on optimizing the parameters of cylindrical gear meshing gears with multi-teeth and high overlapping degree. *Mach. Des. Manuf.* **2021**, *5*, 157–161.
21. Shi, Z.; Jiang, P. Study on numerical simulation algorithm of gear double-flank rolling test. *Tool Eng.* **2006**, *40*, 118–120.
22. *ISO 1328-1; Cylindrical Gears-Iso System of Flank Tolerance Classification-Part 1: Definitions and Allowable Values of Deviations Relevant to Flanks of Gear Teeth*. ISO: Geneva, Switzerland, 2013.
23. Zhang, Z.; Huang, T.; Huang, S.; Kang, D.; Wang, H.; Duan, R.; Xu, L. A new kind of gear measurement technique. *Meas. Sci. Technol.* **1997**, *8*, 715.
24. Xie, H.; Fu, Y.; Feng, G.; Ye, Y.; Huang, W. New way for accuracy measurement of fine-pitch gears in batch production. *Int. Soc. Opt. Photonics* **2011**, 7997, 303–308.
25. Wang, X.; Shu, Z.; Shi, Z. Theoretical method for calculating the unit curve of gear integrated error. *J. Mech. Des.* **2016**, *138*, 033301.
26. Huang, T. A new technology for measuring the dynamic gear integrated error. *Machinery* **1979**, *1*, 1–26.

Disclaimer/Publisher's Note: The statements, opinions and data contained in all publications are solely those of the individual author(s) and contributor(s) and not of MDPI and/or the editor(s). MDPI and/or the editor(s) disclaim responsibility for any injury to people or property resulting from any ideas, methods, instructions or products referred to in the content.